Genetic analysis of hybrid incompatibility suggests transposable elements increase reproductive isolation in the *D. virilis* clade

Dean M. Castillo[*,1] and Leonie C. Moyle[*]

*Department of Biology, Indiana University, Bloomington IN 47405

1. Current address:
School of Biological Sciences, University of Utah, Salt Lake City UT 84112

Running title: TEs contribute to postzygotic isolation

Keywords: Speciation, transposable elements, dysgenesis, Drosophila

Corresponding Author
Dean Castillo
School of Biological Sciences
257 South 1400 E, Room 201
Salt Lake City UT 84112

dean.castillo@utah.edu 801-581-7919

Abstract

Although observed in many interspecific crosses, the genetic basis of most hybrid incompatibilities is still unknown. Mismatches between parental genomes in selfish elements and the genes that regulate these elements are frequently hypothesized to underlie hybrid dysfunction. We evaluated the potential role of transposable elements (TEs) in hybrid incompatibilities by examining hybrids between *Drosophila virilis* strains polymorphic for TEs that cause dysgenesis and a closely related species that appears to lack these elements. Using genomic data, we confirmed copy number differences in potentially causal TEs between the dysgenic-causing *D. virilis* (TE+) strain and a sensitive *D. virilis* (TE-) strain and *D. lummei* genotype. We then contrasted isolation phenotypes in a cross where dysgenic TEs are absent from both *D. virilis* (TE-) and *D. lummei* parental genotypes, to a cross where dysgenic TEs are present in the *D. virilis* (TE+) parent and absent in the *D. lummei* parent, predicting increased reproductive isolation in the latter cross. Using F1 and backcross experiments that account for alternative hypotheses, we demonstrated amplified reproductive isolation specifically in the interspecific cross involving TE+ *D. virilis*, consistent with the action of dysgenesis-inducing TEs. These experiments demonstrate that TEs can contribute to hybrid incompatibilities via presence/absence polymorphisms.

85 **Introduction**

86 Post-zygotic reproductive isolation in hybrid individuals is generally proposed to be a
87 consequence of negative genetic interactions among two or more loci (Dobzhansky 1937; Muller
88 1942). Genic differences are obvious candidates to underlie these hybrid incompatibilities.
89 However because the exact loci involved are known in only a few cases (Johnson 2010;
90 Presgraves 2010; Castillo and Barbash 2017), the importance of other genetic mechanisms in
91 generating hybrid incompatibilities is still undetermined. One alternative mechanism involves
92 the action of selfish genetic elements, including repetitive elements (Michalak 2009; Johnson
93 2010; Werren 2011; Crespi and Nosil 2013). The proposal that transposable elements (TEs)
94 contribute to reproductive isolation was met with early skepticism, largely due to a failure to
95 detect their proposed mutational effects—including increases in the mutation rate—in crosses
96 between different species with marked postzygotic isolation (Coyne 1986; Hey 1988; Coyne
97 1989). However, we now understand that phenotypes related to 'dysgenesis'—a specific
98 incompatibility phenotype caused by TEs—instead reflect more complex effects of de-repression
99 of TE transcription (Martienssen 2010; Khurana *et al.* 2011) and genome wide DNA damage
100 (Khurana *et al.* 2011), rather than strictly mutational effects on essential genes (Petrov *et al.*
101 1995; Blumenstiel and Hartl 2005). This potential to cause negative genetic interactions via TE
102 de-repression in hybrids, places TEs within the classical Dobzhansky-Muller framework for the
103 evolution of incompatibilities (Johnson 2010; Castillo and Moyle 2012; Crespi and Nosil 2013).

104 A role for selfish elements in postzygotic reproductive isolation has been strongly
105 suggested by empirical studies across plants and animals that correlate differences in repetitive
106 elements between species with increased repeat transcription and dysfunction in hybrids
107 (Labrador *et al.* 1999; Martienssen 2010; Brown *et al.* 2012; Dion-Cote *et al.* 2014).

108 Nonetheless there have been few attempts to directly assess the role of TEs in the expression of
109 reproductive isolation. Clades with differences in TE content within and between species can be
110 leveraged to infer the roles of TEs in reproductive isolation by conducting specific crosses that
111 are predicted a priori to display elevated hybrid dysfunction based on the presence or absence of
112 lineage specific TEs. Dysgenic systems in *Drosophila* are among the best characterized in terms
113 of phenotypic effects of TEs that could be relevant to reproductive isolation. Most notable
114 among these, the dysgenic syndrome within *Drosophila virilis* and the *P-element* system within
115 *D. melanogaster* are typically defined by gonad atrophy when a strain carrying transposable
116 elements is crossed with a strain lacking these elements (Kidwell 1985; Lozovskaya *et al.* 1990).
117 The dysgenic phenomenon depends on the direction of the cross—dysgenesis occurs when the
118 female parent lacks the TE elements—and the copy number in the paternal parent (Srivastav and
119 Kelleher 2017; Serrato-Capuchina *et al.* 2020b). These intraspecific dysgenic systems can be
120 used to evaluate the contribution of TEs to reproductive isolation with other species, by
121 contrasting the magnitude of interspecific hybrid dysfunction generated from lines that do and do
122 not carry active dysgenic elements. This contrast requires two genotypes/lines within a species
123 that differ in the presence of specific TEs known to cause dysgenesis in intraspecies crosses, and
124 a second closely related species that lacks these TEs. If the TEs responsible for hybrid
125 dysfunction within a species also influence reproductive isolation, interspecific crosses involving
126 the TE-carrying line should exhibit greater hybrid incompatibility than crosses involving the
127 lines in which TEs are absent.

128 In this study, we evaluate whether TEs with known effects on intraspecific hybrid
129 dysgenesis also affect interspecific reproductive isolation, using the *D. virilis* dysgenic system
130 and the closely related species *D. lummei*. Species in the *D. virilis* clade are closely related,

131 easily crossed with one another, and vary in transposable element abundance with *D. lummei*
132 lacking full length active TEs such as *Penelope* (Zelentsova *et al.* 1999; Evgen'ev *et al.* 2000)
133 and other elements (see below). Dysgenesis was first described within *D. virilis* by Lozovskaya
134 and colleagues (Lozovskaya *et al.* 1990) when they observed gonadal atrophy and sterility in
135 males and females in crosses between strains that vary in transposable elements. Initially one
136 major element, *Penelope,* was implicated in the dysgenic phenotype (Evgenev *et al.* 1997), but
137 more recent studies have inferred that *Penelope* cannot be the causal agent and have proposed
138 other specific elements as the primary cause of dysgenesis (Rozhkov *et al.* 2013; Funikov *et al.*
139 2018; Hemmer *et al.* 2019). Therefore dysgenesis in *D. virilis* may be more complex than
140 described in *D. melanogaster* (Petrov et al. 1995) because several elements might contribute to
141 the phenotype.

142 Using these features and the established role of hybrid dysgenesis among *D. virilis* strains
143 we contrast a cross where dysgenic TEs are absent from both *D. virilis* (TE-) and *D. lummei*
144 parental genotypes to a cross where dysgenic TEs is present in the *D. virilis* (TE+) parent and
145 absent in the *D. lummei* parent, to evaluate the connection between postzygotic reproductive
146 isolation and differences in TE composition. In intraspecific crosses between female *D. virilis*
147 that lack relevant TEs (TE-) and male *D. virilis* that carry these TEs (TE+), strong dysgenesis is
148 observed. Therefore, in interspecific crosses we expect the strongest reproductive isolation
149 specifically between *D. lummei* females that lack dysgenic inducing TEs and *D. virilis* males that
150 are TE+—an asymmetrical pattern that is important to distinguish a model of TEs from
151 alternative explanations. With these expectations, using a series of directed crosses and
152 backcrosses, we infer that patterns of reproductive isolation observed in our study are consistent
153 with a causal role for TEs in the expression of postzygotic species barriers.

154

155 **Materials and Methods**

156 *Fly stocks*

157 Two *D. virilis* stocks were used in the experiments. Strain 9 is a wild type strain that was
158 collected in Georgia, USSR in 1970 and is consistently used as a parent in dysgenic crosses
159 because it lacks inducing repetitive elements (Lozovskaya *et al.* 1990; Blumenstiel and Hartl
160 2005). For the purposes of this study we refer to this strain as TE-. The reference genome strain
161 was used as our inducer strain (UCSD stock number 15010-1051.87) because it is known to
162 induce dysgenesis (Blumenstiel 2014), and we refer to this strain as TE+. The genome strain was
163 used instead of Strain 160, which is commonly used in dysgenic studies, because we experienced
164 significant premating isolation between Strain 160 and *D. lummei* in single pair crosses, that
165 precluded further genetic analysis and examination of postzygotic isolation. The reference
166 genome strain is closely related to Strain 160 as both were created by combining several
167 phenotypic markers to make multiply marked lines (genome strain genotype *b; tb, gp-L2; cd; pe*)
168 (Lozovskaya *et al.* 1990). The strain of *D. lummei* was acquired from the UCSD stock center
169 (15010-1011.07).

170

171 <u>*Estimating copy number of dysgenic causing elements*</u>

172 We used publicly available genomes from several *D. virilis* strains and species in the virilis clade
173 to examine the copy number of potentially dysgenic causing elements. The SRA accession
174 numbers and strain information for all samples are listed in Supplemental Table 1. We focused
175 on candidate TEs that are associated with dysgenesis (Funikov *et al.* 2018) but mapped reads to
176 all inserts from a previously compiled TE library (Erwin *et al.* 2015) to prevent bias that might

177 arise from mapping reads from the other species to a TE library generated from *D. virilis*. All
178 copy number estimates were made using deviaTE (Weilguny and Kofler 2019), which estimates
179 haploid copy number based on single-copy "control" genes. For our control genes we chose the
180 *D. virilis* homologs of Beta-tubulin60D and alpha-tubulin84B as essential single copy genes in
181 the *Drosophila virilis* genome.

182 We first compared copy number differences between the genomes of the inducing strain
183 *D. virilis* Strain 160 and *D. virilis* Strain 9 (TE-), the two strains typically used in studies of
184 dysgenesis. We determined the reliability of our estimates for identifying potentially causal TEs,
185 by comparing our estimate for the enrichment of TE copy in Strain 160 to other studies that have
186 used read mapping abundance from genomic data and read abundance for piRNA from ovaries
187 of each strain (Erwin *et al.* 2015; Funikov *et al.* 2018). Although the majority of work on
188 dysgenesis in *D. virilis* has focused on *Penelope*, new evidence suggests that *Penelope* does not
189 play a role in dysgenesis (Rozhkov *et al.* 2013; Funikov *et al.* 2018). Therefore, we looked at
190 relationships between candidate TEs and *Penelope* across *D. virilis* genomes, to determine which
191 of these TEs had similar copy number distribution as *Penelope*. We specifically focused on
192 *Penelope, Polyphemus, Paris, Helena, Skippy,* and *Slicemaster,* given their greater mapping
193 abundance in inducer vs non-inducer strains (Funikov *et al.* 2018). We used hierarchical
194 clustering to determine the correspondence of copy number of each candidate TE and *Penelope*
195 across strains. A strong correspondence suggests a causal role for this element in the dysgenic
196 studies that have previously focused on *Penelope*.

197 We next determined which candidates had a higher average copy number in the two
198 inducing strains (the genome strain TE+ and 160) compared to the non- inducing Strain 9 (TE-)
199 as well as the copy number average of the two *D. lummei*. We retained the threshold of two-fold

200 increase in the average TE copy number, based on the analysis above. We also examined the
201 differences in allele frequencies and polymorphic sites in the *D. lummei* strains compared to *D.*
202 *virilis* strains. We filtered SNPs using default settings in deviaTE to calculate the average major
203 allele frequency at each site as well as the number of sites that were polymorphic. TEs that are
204 homogenous (have an average major allele frequency close to one) reflect either new invasions
205 or active TEs, whereas evidence for the accumulation of variable sites indicates older inactive
206 elements (Beall *et al.* 2002; Erwin *et al.* 2015; Weilguny and Kofler 2019).
207
208 *Intra- and interspecies crosses to determine the nature of reproductive isolation*
209 Virgin males and females from each stock were collected as they eclosed and aged for seven
210 days prior to matings. All crosses involved single pairs of the focal female and male genotype
211 combination (a minimum of 20, range 20-23, replicates were completed for a given female ×
212 male genotype combination). In total there were three intra-strain crosses that we completed to
213 account for fecundity differences in subsequent analysis (TE- × TE-, TE+ × TE+, and *D. lummei*
214 × *D. lummei*). As expected, in the three intra-strain crosses we did not see any evidence of male
215 or female gonad atrophy (classical dysgenic phenotypes) or skewed sex ratios. There were
216 differences in the total number of progeny produced, hatchability, and proportion of embryos
217 that had reached the pre-blastoderm stage (hereafter 'proportion fertilized'). We used these
218 values as baseline estimates of maternal effects which might influence these phenotypes in
219 subsequent inter-strain analyses (Table 1; Table 2).
220 For inter-strain comparisons, we performed all reciprocal crosses between the three
221 strains to analyze reproductive isolation on F1 progeny. These crosses fell into three categories.
222 **I-Intraspecific Crosses Polymorphic for TEs:** Crosses between TE- and TE+ were used to

223 confirm the expression of intraspecific male dysgenesis when the inducing (TE+) strain was used
224 as a father. **II-Interspecies crosses with no TEs present:** Crosses between TE- and *D. lummei*
225 were used to determine the nature of reproductive isolation between the species in the absence of
226 dysgenic inducing TEs. **III-Interspecies crosses with TEs present:** Crosses between TE+ and
227 *D. lummei* were used to determine the additional contribution, if any, of TEs to interspecific
228 post-mating reproductive isolation (Supplemental Fig 1). This contrast assumes that the two *D.*
229 *virilis* strains, TE- and TE+, do not differ from each other in their genic Dobzhansky-Muller
230 incompatibilities with *D. lummei*, an assumption that we could also evaluate with data from
231 crosses performed using hybrid genotypes (described further below).
232
233 *Backcross design to test models of hybrid incompatibility*
234 We used a set of backcross experiments to compare the fit of several models of hybrid
235 incompatibility to our data for intraspecies dysgenesis and interspecific reproductive isolation.
236 F1 males from TE+ and *D. lummei* crosses were generated in both directions. These specific F1
237 males were created because this genotype was used previously to infer the genetic basis of
238 dysgenesis (Lovoskaya et al. 1990; see below). These F1 males were then backcrossed
239 individually to TE- and *D. lummei* females. We evaluated two main classes of models with
240 fitness data from the resulting BC hybrids. Both classes broadly describe Dobzhansky-Muller
241 incompatibilities, because they involve negative epistatic interactions between loci in the two
242 parental strains, however they differ in whether they assume that the interactions occur between
243 genes or between TEs and TE suppressors.
244 *Comparing observed patterns to theoretical expectations*

245 The phenotypes that we observed for postzygotic reproductive isolation could be the
246 product of several non-mutually exclusive genetic mechanisms. Here we describe the unique
247 predictions that are made by different incompatibility models, focusing on two major classes:
248 models that assume interactions between genes from each parental genome (Genic models) and
249 models that assume an asymmetric copy number of TEs between the parental genomes (TE
250 models).

251 *Genic models of hybrid incompatibilities*

252 The first set of models we compared to our empirical observations assume that alternative
253 alleles at incompatible loci have diverged in each lineage and have a dominant negative
254 interaction in F1 and backcross progeny that carry these alleles (Coyne and Orr 2004). When two
255 unlinked loci are involved we expect to see discrete classes of backcross (BC1) genotypes that
256 exhibit hybrid incompatibilities, specifically half of the progeny would carry the incompatible
257 genotype and half would not (Supplemental Fig. 2). If the hybrid incompatibility is not fully
258 penetrant then, on average, any specific replicate BC1 cross would appear to have half the
259 number of progeny exhibiting the hybrid incompatibility compared to F1s from the cross
260 between the parental species. This provides an expectation for us to compare observed levels of
261 incompatibility between F1 and BC1 crosses (see Statistical Analysis below).

262 We also expanded this general model to include interactions between specific
263 chromosomes (e.g. X-autosome interactions), as well more than two interacting loci. More
264 complex models are described in the Supplemental Information. For our purposes we considered
265 an X-autosome model where there is a negative interaction between the X chromosome of the
266 TE- or *D. lummei* parent and an autosome of the TE+ parent (Supplemental Fig. 3). We
267 considered this specific X-autosome interaction because this generates

268 dysgenesis/incompatibility in both sexes for the intraspecific dysgenic cross (TE- × TE+), but no
269 male gonad dysgenesis/incompatibility in the reciprocal cross, consistent with previous reports
270 (Lozovskaya *et al.* 1990). For models in which higher order (greater than 2 loci) interactions are
271 responsible for the incompatibility observed in the F1s, we would expect to observe a smaller
272 proportion of affected individuals in the backcross compared to the F1 cross (Supplemental
273 Table 2); the specific expected degree of hybrid incompatibility in the backcross depends on the
274 total number of loci required for hybrid incompatibility and the number of loci carried by each
275 parental strain.
276
277 *TE models of hybrid incompatibility*
278 To contrast with genic models of hybrid incompatibility we assessed the fit of our
279 observations to a model is based on transposable element copy number. Under this model we
280 expect asymmetric reproductive isolation in crosses between parental species in F1 crosses, and a
281 reduction of hybrid incompatibilities in the backcross. In particular, if the F1 parent used in the
282 backcross has an intermediate copy number of dysgenic causing TEs that is below a minimum
283 copy number necessary to elicit dysgenesis, then we would expect very low or no hybrid
284 incompatibilities in the backcross. This dosage/copy number effect for the *D. virilis* system was
285 first suggested by Vieira et al. (Vieira *et al.* 1998) and has been supported in the *P*-element
286 system in *D. melanogaster* and *D. simulans* (Serrato-Capuchina *et al.* 2020b). The specific
287 prediction of low or no hybrid incompatibility in backcrosses comes from previous observations
288 in crosses between TE- females and males heterozygous for dysgenic factors (F1 males from
289 TE+ × *D. lummei* crosses), where the progeny are not dysgenic (Lozovskaya et al. 1990). We
290 interpret this observation as indicating that the copy number of dysgenic factors (TEs) in the

291 male parent influences the amount of dysgenesis, and is insufficiently high in F1 males of this
292 cross to cause a dysgenic phenotypic in their offspring. This expectation is not predicted from the
293 genic hybrid incompatibility models.
294
295 *Phenotypes measured to infer dysgenesis and post-zygotic reproductive isolation*
296 The phenotypes that we measured to infer levels of post-zygotic isolation were: egg to adult
297 viability and the total number of progeny produced (both forms of inviability), the sex ratio of
298 resulting progeny, and male gonad atrophy (a form of sterility common in dysgenic systems).
299 These phenotypes were measured in both F1 and backcross experiments and could measure both
300 germline and somatic effects of TEs. After the initial pairing of individuals, the parents were
301 kept for seven days. On day 4 the parental individuals were transferred to a new fresh vial. On
302 day 7 the parents were transferred to a vial that had been previously dyed with blue food coloring
303 to assist counting of eggs. All vials were cleared and parental individuals discarded at day 8. To
304 ensure that we compared progeny of the same age among different crosses, we did not use any
305 progeny from the first three days of the cross because both intra-strain and inter-strain crosses
306 involving *D. lummei* females would often produce few or no progeny within this time. To be
307 used in further analyses, an individual cross must have produced at least 10 progeny over the 4
308 day period (days 4-7).
309 To estimate the total number of progeny produced and their sex ratio we counted the
310 number of male and female progeny from days 4-7. We determined the viability of individuals
311 for each cross by counting the number of eggs in the day 7 vial. We then allowed these eggs to
312 hatch and develop and counted the number of pupae and adults. The number of progeny
313 produced and egg to adult viability gave the same results; since the total number of progeny

314 produced was collected from more replicates and could be summarized by normal distributions
315 we only present those data.
316 To estimate male gonad atrophy we collected all flies that eclosed from days 4-6 of the
317 cross and saved males into new vials that we supplemented with extra yeast paste, with <10
318 males per vial. We aged these flies on yeast for five days before scoring gonad atrophy on a
319 dissecting scope by looking for the presence of atrophied testes (Blumenstiel and Hartl 2005). In
320 crosses between Strain 9 and Strain 160 it has been noted that both, one, or zero testes can be
321 atrophied (Blumenstiel and Hartl 2005). Our estimate for analysis was the proportion of testes
322 atrophied for the total number of testes scored. We also examined female ovary atrophy for a
323 small sample from each interspecies cross but did not observe any atrophy, so we focus
324 exclusively on male gonad atrophy.
325 To determine if differences in viability and total proportion of progeny produced for F1
326 crosses could be explained by differences in embryo lethality, we directly assayed hatchability
327 and also assessed evidence for fertilization versus early embryo defects via embryo staining.
328 First, to assay hatchability we set up population cages consisting of 25 males and 25 females
329 using the same genotype combinations that produced F1s described above (3 replicate
330 populations cages were set up per cross type). Males and females were left in the cages for one
331 week and were given grape agar plates supplemented with yeast culture daily. After the
332 acclimation period, a fresh agar plate was given to each population cage. After 24 hours the
333 plates were replaced (Day 1). All the eggs on the plate were counted. Seventy-two hours later
334 (Day 4) all eggs and larvae on the plate were counted. We calculated hatchability as the
335 proportion of eggs that failed to hatch/total number of eggs. This was confirmed by counting
336 larvae on the plates. The day after plates were collected for the hatchability assay (Day 2)

337 another agar plate was collected (eggs had been oviposited for 24 hours) and embryos were
338 collected, fixed, and stained with DAPI following basic protocols (Rothwell and Sullivan 2000;
339 Rothwell and Sullivan 2007; Ferree and Barbash 2009). Briefly, embryos were collected in a
340 nitex basket using 0.1% Triton X-100 Embryo Wash (7g NaCl, 3mL Triton X, 997 mL H20).
341 Embryos were dechorionated using 50% bleach for 3 minutes and rinsed well with water.
342 Embryos were fixed with 37% formaldehyde and n-Heptane and then vitelline membrane was
343 removed by serially shaking and washing in methanol. To stain embryos they were first
344 rehydrated by rinsing with PBS and then blocked by incubating with PBTB, followed by rinsing
345 with PBS before staining with PBTB+ 1:1000 DAPI for 5 minutes. Embryos were visualized
346 using a fluorescent scope immediately after staining to determine if development had progressed.
347 Embryos were considered to have begun development if we could see nuclei patterns typical of
348 preblastoderm, blastoderm, and gastrula stages. Since we did not score fertilization by co-
349 staining and looking for presence of sperm or whether the second phase of meiosis (formation of
350 polar bodies) had been initiated, we may have missed any very early stage embryo lethality and
351 considered these eggs unfertilized. Thus our estimates of embryo lethality are conservative and
352 they potentially underestimate embryo lethality. All females were dissected after this last embryo
353 collection to confirm they had mated by looking for the presence of sperm stored in the
354 reproductive tract.
355
356 *Statistical analysis*
357 <u>F1 reproductive isolation</u>
358 All analyses were performed in R v3.3.2. For traits measured in the F1 crosses we performed
359 three separate analyses, based on the identity of the female used in the cross.

360 To determine if there were differences in trait values based on the male parent in the cross we
361 used linear and generalized linear models. All models had the form

362 $$y = \mu + \beta_i x_i + \beta_j x_j$$

363 μ represents the trait value for the intra-strain cross. β_i and β_j represent the effect sizes for males
364 that were from different strains/species than the female in the specific analysis. For example,
365 when we analyzed data where TE- was the female parent, β_i could represent the deviation
366 caused by having the TE+ strain as the father and $\beta_j$could represent the deviation caused by
367 having *D. lummei* as the father. For a given phenotype there was significant reproductive
368 isolation when $\beta_i$or β_j was significantly less than zero, indicating lower trait value than the intra-
369 strain cross. In the case of sex-ratio any deviation of the correlation coefficient from zero could
370 be interpreted as sex specific effects. The dysgenesis and total progeny produced variables were
371 analyzed with simple linear regressions. Since the sex ratio data are more accurately represented
372 by binomial sampling we analyzed these data using binomial regression (a generalized linear
373 model).

374 To examine whether there was asymmetry in reproductive isolation for the *D. lummei* and
375 TE+ strain cross, it was necessary to convert these phenotypes into relative values, based on the
376 intra-strain cross. For example, TE+ female × *D. lummei* male measurements can be converted to
377 relative values by finding the difference from the TE+ intra-strain cross average value. These
378 relative measurements were compared in pairwise t-tests.

379

380 <u>Backcross reproductive isolation</u>

381 The results for the backcross experiment were analyzed in the same way as the F1 crosses. We
382 compared phenotypes for crosses based on the female parent. Specifically, we compared the

383 phenotype values for the control TE- (*D. virilis*) intra-strain cross with the crosses between TE-
384 females and TE+ or F1 male genotypes. We then compared the phenotype values for the control
385 *D. lummei* intra-strain cross with the crosses involving *D. lummei* females mated to TE+ or F1
386 male genotypes.

387 For a two locus genic model of incompatibility with a negative interaction in F1 progeny
388 between two unlinked autosomal loci, we predict there would be no sex specific effects
389 (Supplemental Fig. 2). When F1 males are used as parents only ½ of the resulting progeny,
390 regardless of sex, should exhibit the hybrid incompatibility. If the epistatic interaction does not
391 have complete penetrance then the effect size in this BC should be ½ compared to the parental
392 cross. For example if 30% of F1 progeny are dysgenic then only 15% of the backcross progeny
393 are expected to be dysgenic. Under a genic model with an X-autosome interaction between the X
394 chromosome of the TE- parent and an autosome of the TE+ parent, sex specific effects will only
395 be observed in the F1 progeny and not in the backcross (Supplemental Fig. 3). Lastly, for the TE
396 model there are no expected sex-specific effects and the level of incompatibility in the backcross
397 will be the same as the intra-strain control, and significantly less than what is predicted from the
398 genic models of incompatibility. For the gonad atrophy data, we analyzed only the data from the
399 F1 male that carried the X chromosome from TE+ since the other genotype was already
400 determined to not be significantly different from zero (see results). For the data on numbers of
401 progeny produced, we pooled all backcrosses for this analyses since they produced the same
402 number of progeny on average (see results).

403

404 <u>Comparison of hatchability and embryo development measurements</u>

405 Any decrease in progeny production could be the result of different mechanisms (prezygotic or
406 postzygotic isolation or both) depending on the specific cross. To determine if lower hatchability
407 was a product of unfertilized eggs (prezygotic isolation) or embryo lethality (postzygotic
408 isolation), we compared these independent measures using contingency tables. We used the
409 proportion of eggs that had begun development past the pre-blastoderm stage as our measure of
410 fertilization rate. Since there were few eggs for a given embryo collection replicate, we pooled
411 across all three replicates. We then compared the proportion of eggs hatching to the proportion of
412 eggs fertilized using a Chi-square test of independence. We could also compare differences in
413 the proportion of eggs fertilized between crosses that shared a common female genotype, to infer
414 premating isolation.
415
416 *Data availability*
417 All data and R code used is available through dryad (doi to be determined).
418
419 **Results**
420 *Estimates of copy number and divergence in dysgenic causing TEs*
421 We confirmed that candidate dysgenic TE copy numbers were consistently different
422 between Strain 160 (TE+) and Strain 9 (TE-) as expected (Erwin *et al.* 2015; Funikov *et al.*
423 2018). Specifically *Penelope, Polyphemus, Paris, Helena, Skippy,* and *Slicemaster* were
424 enriched in Strain 160 compared to Strain 9 (Fig 1A). Using hierarchical clustering across the *D.*
425 *virilis* strains we determined *Polyphermus* had a similar copy number distribution as *Penelope*
426 and formed a cluster that did not include the other candidate TEs (Fig. 1B). The correlation in
427 copy number between *Penelope* and *Polyphemus* across strains was r=0.68 (Fig. 1C, P=0.0073).

428 When one outlier (Dvir87) was removed the correlation increased to r=0.866 (P=0.0001). Either
429 correlation indicates a strong relationship between copy number of these two elements.
430 Using our copy number estimates, we identified two elements, *Polyphemus* and
431 *Slicemaster*, but not *Penelope*, that had higher average copy number in the inducing *D. virilis*
432 strains , Genome Strain (TE+) and Strain 160, compared to the non-inducing *D. virilis* Strain 9
433 (TE-) and two *D. lummei* strains. Interestingly, we were able to find copies of *Penelope* in the *D.*
434 *lummei* genome despite previous reports of the absence of this element (Zelentsova *et al.* 1999).
435 We used the patterns of allele frequency to assess the likelihood that *Polyphemus* and
436 *Slicemaster* were active in inducing strains but not in non-inducing strains. We expected active
437 elements to have homogenous insertions with very few polymorphic sites (Erwin et al. 2015).
438 The pattern for *Polyphemus* was consistent with our expectation for the inducing *D. virilis* strains
439 and non-inducing *D. virilis* strain, although there was a difference in the estimates between the
440 *D. lummei* samples (Supplemental Fig. 4)—one *D. lummei* sample was nearly identical to the
441 non-inducing Strain 9 (TE-), while the other strain had a higher CN and average major allele
442 frequency. Nonetheless, both factors were still lower in both *D. lummei* samples than in the
443 inducing strains (Supplemental Fig. 4). In contrast, the major allele frequency data for
444 *Slicemaster* was consistent with recent broad invasion the *D. virilis* clade because all strains,
445 with the exception of one *D. lummei* strain, had high average major allele frequency. As a result,
446 for *Slicemaster*, there was no consistent pattern differentiating inducing *D. virilis* and non-
447 *inducing D. virilis*, making it an unlikely candidate contributing to dysgenesis.
448 Combined, our observations from within *D. virilis* and comparison between *D. virilis* and
449 *D. lummei* suggest that copy number differences in *Polyphemus* have the potential to play

450 important roles in hybrid dysgenesis. This is consistent with analysis that suggest *Polyphemus*
451 induced DNA breaks in dysgenic progeny (Hemmer *et al.* 2019).
452
453 *Dysgenesis confirmed in intraspecies crosses polymorphic for TEs*
454 In the classic dysgenic cross (TE- female × TE+ male) we observed 38% testes atrophy (Fig. 2).
455 This frequency of gonad atrophy was significantly greater than the TE- intra-strain cross
456 (β=0.3807; P<0.0001). In the reciprocal non-dysgenic cross (TE+ female × TE- male) we
457 observed rare gonad atrophy events at a frequency not significantly different from zero. The non-
458 dysgenic cross produced significantly more offspring than the TE- female × TE- male intra-strain
459 comparison (β=26.732; P=0.0136); this increased productivity may reflect some outbreeding
460 vigor between these long-established lab lines. The number of fertilized eggs differed between
461 crosses so comparing the number that were actually fertilized was critical. There was no
462 deviation in the proportion of eggs hatching compared to the proportion fertilized in either cross,
463 indicating there was no embryo inviability (Table 2).
464
465 *Prezygotic isolation occurs in interspecies crosses when TEs are absent*
466 The TE- × *D. lummei* cross produced, on average, 22 fewer adult progeny than the TE- intra-
467 strain control cross (μ=123.318; P<0.0001; β=-22.509; P=0.0341). This reduction in progeny
468 production likely represents reduced fertilization and prezygotic isolation rather than reduced F1
469 embryo viability in this cross, based on data from two comparisons. First a comparison of the
470 proportion of fertilized embryos to the proportion of embryos hatching within this cross shows
471 that these did not differ, indicating no evidence for embryo lethality. Second, we compared the
472 proportion of fertilized embryos between this cross and the intra-strain control, and found that

473 the proportion of fertilized embryos was significantly less for the TE- × *D. lummei* cross
474 compared to the TE- intra-strain control cross (Table 2), consistent with a prezygotic fertilization
475 barrier.
476 In comparison, the reciprocal cross (*D. lummei* female × TE-) had no evidence of
477 prezygotic isolation or F1 embryo lethality. We actually observed a higher proportion of hatched
478 embryos compared to our estimate for proportion fertilized; this likely reflects an underestimate
479 of fertilization rate because this measure relies on handling embryos with multiple washing and
480 fixing steps which can lead to loss of embryos in the final sample (Rothwell and Sullivan
481 2007b). In contrast to prezygotic isolation, gonad atrophy was not observed for males or females
482 in either reciprocal cross between TE- and *D. lummei*.
483
484 *Strong F1 postzygotic isolation occurs in interspecies crosses when TEs are present*
485 The cross between TE+ females and *D. lummei* males produced rare male gonad atrophy,
486 at frequencies similar to the intraspecies non-dysgenic cross. We also saw no atrophy in the
487 reciprocal *D. lummei* × TE+ cross where gonad atrophy might be expected (Fig 2). Instead,
488 reduced viability was observed in both the reciprocal crosses, resulting in significantly fewer
489 progeny produced compared to control crosses (Fig 3). The TE+ female × *D. lummei* male cross
490 produced 19 fewer progeny compared to the TE+ intra-strain control cross (mu=50.52;
491 P<0.0001; β=-31.37; P<0.0001). In the reciprocal cross, *D. lummei* female × TE+ male, 17
492 fewer progeny were produced compared to the *D. lummei* control cross (mu=34.50; P<0.0001;
493 β=-16.95; P=0.0027). To test for asymmetrical effects, we compared the relative reduction in
494 viability in these reciprocal crosses, taking into account the differences in intra-strain and
495 maternal effects. For the TE+ female × *D. lummei* male cross, progeny production was reduced

496 by 62%; for the reciprocal cross (*D. lummei* × TE+) progeny production was reduced by 50%.
497 These reductions were not significantly different from one another (t=1.547; df=41;P=0.1527).
498 In both crosses involving *D. lummei* and TE+, the proportion of embryos hatched was
499 significantly lower than the proportion of embryos fertilized, indicating that the reduced number
500 of progeny was due to early embryo lethality in both cases (Table 2). In contrast, in the TE+
501 female × *D. lummei* male cross only, inviability was also specifically increased for males,
502 resulting in a significant excess of females and a sex ratio that was 63% female (β=0.1171;
503 P<0.0001; Fig 3).
504 Together our data for F1s suggested that there are possibly two mechanisms contributing
505 to hybrid incompatibilities in this pair. The TE model alone predicts asymmetric reproductive
506 isolation—specifically reduced F1 fitness in the TE+ female × *D. lummei* male cross—so our
507 observation of F1 inviability in both directions suggests an additional mechanism contributing in
508 reciprocal direction, that we also further dissected with crosses (below). This deficit of males is
509 not consistent with an X-autosome incompatibility between the *D. lummei* X and the TE+
510 autosome, because the males that are inviable carry the TE+ X chromosome.
511
512 *Backcross experiments support a role for TEs in postzygotic isolation*
513 Using data on gonad atrophy and hybrid inviability in our backcrosses, we aimed to
514 determine whether the observed patterns of hybrid incompatibility were more consistent with a
515 TE model or genic incompatibility models (Supplemental Fig. 2 and 3). First we assessed the
516 relationship between TE dosage and gonad atrophy with the specific strains used in this
517 experiment by testing whether F1 males from crosses between *D. lummei* and TE+ produced
518 dysgenic sons when crossed to TE- females (similar to Lovoskaya et al. 1990). For the TE model

519 we would expect to observe rescue of gonad atrophy in a backcross using F1 males because these
520 males will have fewer TEs than required to cause dysgenesis. For the genic incompatibility
521 models we would expect this backcross to have half the amount of gonad atrophy observed in the
522 F1s, because only 1/2 of their progeny would carry both incompatible alleles. The 38% F1 gonad
523 atrophy we observed the classic intraspecific dysgenic cross (TE- × TE+ cross) served as our
524 baseline expectation. We found that both backcrosses had significantly less than 19% gonad
525 atrophy, results that are inconsistent with the two locus genic models. When F1 males carried
526 the X chromosome from *D. lummei* the level of dysgenesis was not significantly different than
527 zero (β=0.0264; P=0.1366). When F1 males carried the X chromosome from TE+ the level of
528 dysgenesis was ~6%, significantly less than the TE+ parent (β=0.0638; P=0.0011; CI= 0.0261,
529 0.1016) and less than 19% atrophy. Therefore data for gonad atrophy in our backcrosses are
530 consistent with strong rescue of fertility predicted from the TE incompatibility model.
531 Given our results for gonad atrophy we proceeded to examine support for the different
532 incompatibility models in explaining the other hybrid phenotype—inviability, including sex-
533 specific inviability—we had observed in the interspecies crosses, using similar logic as for the
534 gonad atrophy phenotype. Specifically, we examined progeny production and sex ratio in
535 backcrosses between *D. lummei* females and F1 males. For the TE copy number model we
536 expect rescue of progeny viability when either F1 male is used as the male parent, and no sex
537 specific lethality. For an autosome-autosome model or X-autosome model, we expect to observe
538 ~26 progeny produced, which is ½ of the reduction in progeny observed when comparing the *D.*
539 *lummei* female × TE+ male control cross (where ~17.5 progeny were produced) to the intrastrain
540 control cross (where ~34.5 progeny were produced). In both backcrosses the number of progeny
541 produced was not significantly different than the *D. lummei* × *D. lummei* control cross and

542 represents complete rescue of viability. The strength of this rescue is consistent with the TE copy
543 number model but not the two-locus incompatibility model (Table 3; Fig 3). Using a one-sample
544 *t-test* we determined that both the F1 male carrying the *D. lummei* X chromosome (mean=39.76,
545 se=5.26) and the F1 male carrying the X chromosome from the TE+ (mean=38.41,se=5.56)
546 produced significantly more progeny when crossed with the *D. lummei* female than the expected
547 26 progeny under the two-locus incompatibility model (Table 3).

548 Two-locus genic incompatibility models might be an oversimplification when
549 considering hybrid incompatibilities, so we also considered models with higher order (greater
550 than two independent/freely-recombining loci). For a three-locus autosomal interaction the
551 greatest expected rescue would be 1/4 of the original effect (therefore 9.5% dysgenesis with TE-
552 females and ~30.26 progeny produced with D. *lummei* females), while for a four-locus
553 autosomal interaction the largest rescue would be 1/8 the original effect (4.75% dysgenesis with
554 TE- females and 32.38 progeny produced with *D. lummei* females) (Supplemental Table 2).
555 Using a one sample t-test we rejected the hypothesis that our data can be explained by a three-
556 locus incompatibility for gonadal dysgenesis (H0: μ<9.5; t= -627.2, df = 10, P< 0.0001) and for
557 number progeny produced (H0: μ>30.26; t=2.36, df=28, P=0.0126). We were also able to reject
558 the hypothesis for the four-locus incompatibility for gonadal dysgenesis (H0: μ<4.75; t= -311.48,
559 df = 10, P<0.0001) and number progeny produced (H0: μ >32.38; t=1.802, df=28, P=0.041). We
560 did not explore interactions beyond four loci because *D. virilis* only has four major autosomes
561 and, since we used F1 males that lack recombination, each chromosome is transmitted as a single
562 locus in our crosses.

563 In addition to progeny production, we also had data on sex ratio in our backcrosses.
564 Interestingly, in the cross involving *D. lummei* females and F1 males that carried the X

565 chromosome from TE+ there was a significant deviation from 50% female sex ratio (β =0.25;
566 p=0.037). This deviation could be caused by a hybrid incompatibility, however neither the TE
567 incompatibility model or the specific X chromosome incompatibility model we considered
568 predicted sex-specific effects past the F1 generation (see methods). Since we had already
569 observed a pattern of sex-specific inviability from the cross between TE+ females and *D. lummei*
570 males, we also used the backcross data to determine the genetic factors responsible for this
571 additional male-specific hybrid inviability. The only two other crosses where we observed a
572 skewed sex ratio were also female-biased and involved F1 males that carried the X chromosome
573 from TE+ and *D. lummei* Y crossed with *D. lummei* or TE- females (Fig. 4). In each of these
574 three crosses, males had different X chromosome genotypes but consistently had the *D. lummei*
575 Y chromosome. From this, we conclude that this additional incompatibility is caused by an
576 autosome-Y interaction.
577
578 **Discussion**
579 In this study, we used a powerful set of crosses to test whether the presence of TEs with
580 known effects on intraspecies hybrid dysgenesis also influences reproductive isolation. Using the
581 *D. virilis* dysgenic system we predicted that the *D. virilis* strain carrying dysgenic-inducing TEs
582 should show increased reproductive isolation when crossed with *D. lummei* lacking these TEs,
583 compared to the cross involving the *D. virilis* strain that lacks dysgenic-inducing TEs. Taken
584 together, our genetic data support the inference that TEs contribute to elevated reproductive
585 isolation observed in the interspecific cross that involves dysgenic TEs, and are inconsistent with
586 alternative hybrid incompatibility models to explain this elevated isolation. In addition, with
587 genomic data we also assessed which candidate TE might be responsible for observed dysgenesis

588 patterns among inducing *D. virilis* strains compared to non-inducing *D. virilis* and *D. lummei*,
589 and confirmed *Polyphemus* as a strong candidate (Funikov *et al.* 2018; Hemmer *et al.* 2019).
590 A role for accumulated selfish genetic elements in the expression of postzygotic
591 reproductive isolation is consistent with the Dobzhansky-Muller model of hybrid incompatibility
592 (Johnson 2010; Castillo and Moyle 2012; Crespi and Nosil 2013), but little emphasis has been
593 placed on the difficulty of disentangling the effects of these selfish elements from the effects of
594 other hybrid incompatibilities. For example, one way TEs are thought to contribute to
595 reproductive isolation is through transcriptional misregulation that causes sterility or inviability
596 (Martienssen 2010; Michalak 2010; Dion-Cote *et al.* 2014). However, this is not a unique feature
597 of TE-based hybrid incompatibility; divergence in trans and cis-regulatory elements are common
598 and can also cause misregulation and hybrid incompatibilities (reviewed in (Mack and Nachman
599 2017)). To disentangle TE-specific from other effects it would therefore also be necessary to
600 differentiate whether TE misregulation is symptomatic of a common misregulation phenomena
601 in hybrids or if TE divergence drives global misregulation. Instead of focusing on analyzing
602 patterns of misregulation, here we took the approach of isolating phenotypic effects due to TEs
603 by using strains with defined differences in TE abundance, and potential activity, making explicit
604 predictions about which hybrid classes should exhibit increased reproductive isolation, and
605 evaluating these using classical genetic crosses.
606 The strength of this approach relies on our ability to make and test predictions that are
607 exclusive to a TE incompatibility model, compared to alternative genic models, and thereby
608 differentiate effects due to TE- and non-TE causes. For example, we observed that postzygotic
609 incompatibility occurred only in crosses involving the TE-carrying *D. virilis* strain, and not in the
610 cross between TE- *D. virilis* and *D. lummei,* clearly implicating the presence of TEs in this

611 postzygotic isolation. For all of these incompatibilities to instead be genic would require that
612 they all happened to accumulate in the TE-carrying *D. virilis* strain, a scenario that is possible in
613 principle but biologically implausible. Nonetheless, the observation of equally strong
614 postzygotic isolation in both directions of the cross does suggest the additional contribution of
615 other non-TE factors between our *D. virilis* TE+ line and *D. lummei*.

616 Our ability to disentangle the effects of TEs vs non-TE incompatibilities in backcross
617 offspring rested on the observation that F1 males failed to produce dysgenic sons when crossed
618 to TE- females (Lovoskaya et al. 1990). The mechanism we propose based on previous studies
619 (Vieira *et al.* 1998; Srivastav and Kelleher 2017; Serrato-Capuchina *et al.* 2020b), is that F1s
620 have sufficiently low copy number of TEs such that dysgenesis does not occur when F1 males
621 are themselves used as fathers. This pattern allowed us to compare the TE incompatibility model
622 with genic incompatibility models because they make contrasting predictions about the level of
623 incompatibility expected. We found that both the rescue of non-atrophied testes in crosses
624 between TE- females and F1 males, and the rescue of viability in crosses between *D. lummei*
625 females and F1 males, is consistent with the TE incompatibility model; significantly greater
626 rescue was observed in these crosses than predicted by the genic incompatibility models. Using
627 these backcrosses we were also able to determine that additional non-TE loci contributed to the
628 incompatibility observed in the TE+ × *D. lummei* cross. This inviability was male specific,
629 suggested by a female biased sex ratio, and resulted from an autosome-Y incompatibility.
630 Together these observations support the operation of two distinct mechanisms of hybrid
631 inviability in our crosses, one of which directly implicates TEs in the expression of this
632 postzygotic isolating barrier.

633 A second inference from our results is that TEs can cause different hybrid incompatibility
634 phenotypes—that is, sterility or inviability—depending on context. TEs misregulation can cause
635 substantial cellular or DNA damage which has the potential to produce multiple different
636 incompatibility phenotypes (Tasnim and Kelleher ; Phadnis N. *et al.* 2015). Although the
637 mechanistic link between damage and hybrid incompatibility needs further exploration, these
638 observations suggest that the occurrence of hybrid sterility vs hybrid inviability could result from
639 misregulation of the same TEs at different developmental stages. Moreover, while transposable
640 elements have typically been thought to restrict their damage to the germline, this is not always
641 the case, including in the dysgenic *D. virilis* system. For example, direct evidence that TEs that
642 can cause inviability phenotypes when active in somatic tissue comes from a *P-element* mutant
643 that was engineered to have expression in somatic cells (Engels *et al.* 1987); in this case,
644 inviability that is dependent on *P*-element copy number was observed in crosses involving this
645 somatically-expressed *P-element* mutant line. Overall, it is mechanistically plausible that this
646 element is responsible for both of our observed incompatible phenotypes. The involvement of
647 TEs in both germline and somatic effects in hybrids would provide a potentially direct
648 mechanistic connection between the effects of a molecular change (the accumulation of TEs) and
649 both intraspecies dysgenesis and interspecies reproductive isolation.
650 Finally, our observations also identify a mechanism that could contribute to variation
651 among intraspecific strains in the strength of their isolation from other species. Evidence for
652 polymorphic incompatibilities is typically inferred from the observation that there is among-
653 population variation in isolation phenotypes when crossed with a second species, because the
654 specific alleles underlying this variation is usually unknown (Reed and Markow 2004;
655 Kozlowska *et al.* 2012). These polymorphic incompatibility loci are typically assumed to be

656 based on genic Dobzhansky-Muller incompatibilities (Cutter 2012). In this study, we show that
657 the presence/absence of TEs segregating in populations and species can also contribute to
658 intraspecific variation in the strength of isolation between species. Moreover, the rapid pace with
659 which TE abundance and identity can change within a lineage also indicates that such differences
660 could rapidly accumulate between species; this suggests that this mechanism is most likely to
661 influence species pairs in which there is dynamic turnover in the identity of their active TEs.
662 Overall, here we have provided evidence for a role of TEs in increased reproductive
663 isolation between lineages that differ in the presence of specific active TE families, by
664 leveraging known TE biology to differentiate TE vs non-TE effects in a set of targeted crosses.
665 The generality of when and how TEs contribute to reproductive isolation could be further
666 addressed by similarly focusing on other *a priori* cases where species are known to vary in the
667 number or identity of TEs, rather than relying on interpreting patterns of TE misregulation that
668 arise in hybrid crosses. For instance, increased reproductive isolation cause by transposable
669 elements was recently reported in crosses between *D. simulans*, that are polymorphic for *P-*
670 *elements*, and a sister species, *D. sechellia*, that completely lack *P-elements* (Serrato-Capuchina
671 et al. 2020a). Moreover, studies that examine lineages at a range of stages of TE differentiation
672 would be particularly valuable for addressing the contribution of TEs to the accumulation of
673 hybrid incompatibilities over evolutionary time. Our findings suggest that the rapid evolution of
674 TEs in different lineages could potentially explain the presence of polymorphic incompatibilities
675 in many systems that experience dynamic changes in these selfish genetic elements.
676
677
678 **Literature Cited**
679
680 Beall, E. L., M. B. Mahoney and D. C. Rio, 2002 Identification and analysis of a hyperactive
681 mutant form of Drosophila P‐element transposase. Genetics 162**:** 217-227.

682 Blumenstiel, J. P., 2014 Whole genome sequencing in *Drosophila virilis* identifies *Polyphemus*,
683 a recently activated Tc1-like transposon with a possible role in hybrid dysgenesis. Mobile
684 DNA 5**:** 6.
685 Blumenstiel, J. P., and D. L. Hartl, 2005 Evidence for maternally transmitted small interfering
686 RNA in the repression of transposition in *Drosophila virilis*. Proceedings of the National
687 Academy of Sciences of the United States of America 102**:** 15965-15970.
688 Brown, J. D., V. Piccuillo and R. J. O'Neill, 2012 Retroelement Demethylation Associated with
689 Abnormal Placentation in Mus musculus x Mus caroli Hybrids. Biology of Reproduction
690 86**:** NIL_0272-NIL_0281.
691 Castillo, D., and L.C. Moyle, 2012 Evolutionary implications of mechanistic models of TE-
692 mediated hybrid incompatability. International Journal of Evolutionary Biology 2012.
693 Castillo, D. M., and D. A. Barbash, 2017 Moving speciation genetics forward: modern
694 techniques build on foundational studies in *Drosophila*. Genetics 207**:** 825-842.
695 Coyne, J. A., 1986 Meiotic segregation and male recombination in interspecific hybrids of
696 *Drosophila*. Genetics 114**:** 485-494.
697 Coyne, J. A., 1989 Mutation rates in hybrids between sibling species of *Drosophila*. Heredity 63**:**
698 155-162.
699 Coyne, J. A., and H. A. Orr, 2004 *Speciation*. Sinauer Associates.
700 Crespi, B., and P. Nosil, 2013 Conflictual speciation: species formation via genomic conflict.
701 Trends in Ecology & Evolution 28**:** 48-57.
702 Cutter, A. D., 2012 The polymorphic prelude to Bateson-Dobzhansky-Muller incompatibilities.
703 Trends in Ecology & Evolution 27.
704 Dion-Cote, A. M., S. Renaut, E. Normandeau and L. Bernatchez, 2014 RNA-seq Reveals
705 Transcriptomic Shock Involving Transposable Elements Reactivation in Hybrids of
706 Young Lake Whitefish Species. Molecular Biology and Evolution 31**:** 1188-1199.
707 Dobzhansky, T., 1937 *Genetics and the Origin of Species*. Columbia University Press.
708 Engels, W. R., W. K. Benz, C. R. Preston, P. L. Graham, R. W. Phillis *et al.*, Somatic effects of
709 *P* element activity in *Drosophila melanogaster:* pupal lethality. Genetics 117**:** 745-757.
710 Erwin, A. A., M. A. Galdos, M. L. Wickersheim, C. C. Harrison, K. D. Marr *et al.*, 2015 piRNAs
711 are associated with diverse transgenerational effects on gene and transposon expression
712 in a hybrid dysgenic syndrome of *D. virilis*. Plos Genetics 11**:** e1005332.
713 Evgen'ev, M. B., H. Zelentsova, H. Poluectova, G. T. Lyozin, V. Veleikodvorskaja *et al.*, 2000
714 Mobile elements and chromosomal evolution in the virilis group of Drosophila.
715 Proceedings of the National Academy of Sciences of the United States of America 97**:**
716 11337-11342.
717 Evgenev, M. B., H. Zelentsova, N. Shostak, M. Kozitsina, V. Barskyi *et al.*, 1997 Penelope, a
718 new family of transposable elements and its possible role in hybrid dysgenesis in
719 Drosophila virilis. Proceedings of the National Academy of Sciences of the United States
720 of America 94**:** 196-201.
721 Ferree, P. M., and D. A. Barbash, 2009 Species-specific heterochromatin prevents mitotic
722 chromosome segregation to cause hybrid lethality in *Drosophila*. Plos Genetics 7**:**
723 e10000234.
724 Funikov, S. Y., D. A. Kulikova, G. S. G.S. Krasnov, A. P. A.P. Rezvykh, L. N. L.N. Chuvakova
725 *et al.*, 2018 Spontaneous gain of susceptibility suggests a novel mechanism of resistance
726 to hybrid dysgenesis in *Drosophila virilis*. Plos Genetics 14**:** e1007400.

727 Hemmer, L. W., G. Dias, B. Smith, K. Van Vaerenberghe, A. Howard *et al.*, 2019 The meiotic
728 recombination landscape of Drosophila virilis is robust to mitotic damage during hybrid
729 dysgenesis. bioRxiv https://doi.org/10.1101/342824.
730 Hey, J., 1988 Speciation via hybrid dysgenesis: Negative evidence from the *Dorosophila affinis*
731 subgroup. Genetica 78**:** 97-104.
732 Johnson, N. A., 2010 Hybrid incompatibility genes: remnants of a genomic battlefield? Trends in
733 Genetics 26**:** 317-325.
734 Khurana, J. S., J. Wang, J. Xu, B. S. Koppetsch, T. C. Thomson *et al.*, 2011 Adaptation to *P*
735 *element* transposon invasion in *Drosophila melanogaster*. Cell 147**:** 1551-1563.
736 Kidwell, M. G., 1985 Hybrid dysgenesis in *Drosophila melanogaster*: nature and inheritance of
737 P-element regulation. Genetics 111**:** 337-350.
738 Kozlowska, J. L., A. R. Ahmad, E. Jahesh and A. D. Cutter, 2012 Genetic variation for post-
739 zygotic reproductive isolation between *Caenorhabditis briggsae* and *Caenorhabditis sp.*
740 *9*. Evolution 66**:** 1180-1195.
741 Labrador, M., M. Farre, F. Utzet and A. Fontdevila, 1999 Interspecific hybridization increases
742 transposition rates of Osvaldo. Molecular Biology and Evolution 16**:** 931-937.
743 Lozovskaya, E. R., V. S. Scheinker and M. B. Evgenev, 1990 A hybrid dysgenesis syndrome in
744 *Drosophila virilis*. Genetics 126.
745 Mack, K. L., and M. W. Nachman, 2017 Gene regulation and speciation. Trends in Genetics 33**:**
746 68-80.
747 Martienssen, R., 2010 Heterochromatin, small RNA and post-fertilization dysgenesis in
748 allopolyploid and interploid hybrids of *Arabidopsis*. New Phytologist 186**:** 46-53.
749 Michalak, P., 2009 Epigenetic, transposon and small RNA determinants of hybrid dysfunctions.
750 Heredity 102**:** 45-50.
751 Michalak, P., 2010 An eruption of mobile elements in genomes of hybrid sunflowers. Heredity
752 104**:** 329-330.
753 Muller, H. J., 1942 Isolationg mechanisms, evolution and temperature. Biological Symposia 6**:**
754 71-125.
755 Petrov, D. A., J. L. Schutzman, D. L. Hartl and E. R. Lozovskaya, 1995 Diverse transposable
756 elements are mobilized in hybrid dysgenesis in *Drosophila virilis*. Proceedings of the
757 National Academy of Sciences of the United States of America 92**:** 8050-8054.
758 Phadnis N., E. P. E. P. Baker, J. C. J. C. Cooper, K. A. K. A. Frizzell, E. E. Hsieh *et al.*, 2015 An
759 essential cell cycle regulation gene causes hybrid inviability in *Drosophila*. Science 350**:**
760 1552-1555.
761 Presgraves, D. C., 2010 The molecular evolutionary basis of species formation. Nature Reviews
762 Genetics 11**:** 175-180.
763 Reed, L. K., and T. A. Markow, 2004 Early events in speciation: polymorphism for hybrid male
764 sterility in Drosophila. Proceedings of the National Academy of Sciences of the United
765 States of America 101**:** 9009-9012.
766 Rothwell, W. F., and W. Sullivan, 2000 Flourescent analysis of *Drosophila* embryos in
767 *Drosophila Protocols*, edited by S. e. al. Cold Springs Harbor Laboratory Press, Cold
768 Springs Harbor, NY.
769 Rothwell, W. F., and W. Sullivan, 2007 Drosophila embryo collection. Cold Spring Harbor
770 Protocols Sep 1.

771 Rozhkov, N. V., N. G. Schostak, E. S. Zelentsova, I. A. Yushenova, O. G. Zatsepina *et al.*, 2013
772 Evolution and dynamics of small RNA response to a retroelement invasion in
773 *Drosophila*. Molecular Biology and Evolution 30**:** 397-408.
774 Serrato-Capuchina, A., E.R.R. D'Agostino, D. Peede, B. Roy, K. Isbell *et al*., 2020a *P*-elements
775 strengthen reproductive isolation within the *Drosophila simulans* species complex.
776 bioRxiv https://doi.org/10.1101/2020.08.17.254169.
777 Serrato-Capuchina, A., J. Wang, E. Earley, D. Peede, K. Isbell *et al.*, 2020b Paternally inherited
778 *P-element* copy number affects the magnitude of hybrid dysgenesis in *Drosophila*
779 *simulans* and *D. melanogaster*. Genome Biology and Evolution 12**:** 808-826.
780 Srivastav, S. P., and E. S. Kelleher, 2017 Paternal induction of hybrid dysgenesis in *Drosophila*
781 *melanogaster* is weakly correlated with both *P-element* and *hobo* element dosage. G3 7**:**
782 1487-1497.
783 Tasnim, S., and E. S. Kelleher, *p53* is required for female germline stem cell maintenance in *P*-
784 element hybrid dysgenesis. Developmental Biology 434**:** 215-220.
785 Vieira, J., C. P. Vieira, D. L. Hartl and E. R. Lozovskaya, 1998 Factors contributing to the hybrid
786 dysgenesis syndrome in Drosophila virilis. Genetical Research 71**:** 109-117.
787 Weilguny, L., and R. Kofler, 2019 DeviaTE: assembly-free analysis and visualization of mobile
788 genetic element composition. Molecular Ecology Resources 19**:** 1346-1354.
789 Werren, J. H., 2011 Selfish genenetic elements, genetic conflict, and evolutionary innovation.
790 Proceedings of the National Academy of Sciences of the United States of America 108**:**
791 10863-10870.
792 Zelentsova, H., H. Poluectova, L. Mnjoian, G. Lyozin, V. Veleikodvorskaja *et al.*, 1999
793 Distribution and evolution of mobile elements in the *virilis* species group of *Drosophila*.
794 Chromosoma 108**:** 443-456.
795
796

797

Table 1. Average trait means for control intrastrain crosses. These values are used as baseline in statistical models testing for increased reproductive isolation in interspecis crosses. For male dysgensis (n) refers to the number of male progeny scored. se=standard error. The number of replicates used to calculate the standard error are n=22 (TE-), n=23 (TE+), and n=20 (*D. lummei*)

Female	Male	Dysgenesis (n)	Sex Ratio (se)	Viability (se)
TE-	TE-	0.0 (1398)	0.488 (0.016)	0.844 (0.055)
TE+	TE+	0.0 (575)	0.516 (0.014)	0.571 (0.057)
D. lummei	*D. lummei*	0.0 (335)	0.521 (0.015)	0.411 (0.067)

Table 2. F1 postzygotic reproductive isolation, as observed in crosses between TE+ and *D. lummei,* is a product of embryo inviability. Inviability is inferred when fewer eggs hatch than expected based on the proprtion of eggs that initiated development (proportion fertilized). The samples sizes (n) are the pooled number of embryos examined across replicate crosses. * represents significant differences in the proportion fertilized from proportion hatched. † represents a significant difference in the proportion fertilized for an interspecific cross compared to the control cross of the maternal strain.

Female	Male	Proportion Fertilized (n)	Proportion Hatched (n)	χ_1^2
TE-	TE-	0.85 (179)	0.79 (344)	2.76
TE+	TE+	0.58 (155)	0.55 (224)	0.2
D. lummei	*D. lummei*	0.61 (218)	0.67 (260)	1.75
TE-	TE+	0.85 (180)	0.80 (283)	1.00
TE+	TE-	0.57 (153)	0.57 (206)	0.00
TE-	*D. lummei*	0.33† (389)	0.39 (79)	0.59
D. lummei	TE-	0.60 (161)	0.75 (337)	12.18*
TE+	*D. lummei*	0.55 (126)	0.42 (235)	5.41*
D. lummei	TE+	0.43† (212)	0.31 (208)	6.06*

Table 3. Progeny production is rescued when F1 males are crossed to *D. lummei* females. For the backcrosses we tested whether progeny rescue was greater than the expectation for two locus genic incompatibility models. F1-1 are males from the *D. lummei* × TE+ cross and F1-2 males are from the reciprocal cross. For the progeny produced we report the number of replicate crosses (n) and the standard error (se). *indicates a significant difference in progeny production from the intrastrain control.

Female	Male	Mean Progeny Produced (n, se)	*t* statistic H0: mu=26 (df)	*P*-value
D. lummei	*D. lummei*	34.50 (20, 4.28)	NA	NA
D. lummei	TE+	17.54* (22, 2.78)	NA	NA
D. lummei	F1-1	39.76 (17,5.26)	2.61 (16)	0.009
D. lummei	F1-2	38.41 (12, 5.56)	2.22 (11)	0.023

822 **Figure 1.** Identification of dysgenic causing transposable elements in *D. virilis*. A) Candidate
823 TEs have higher copy number in the inducing Strain 160 compared to the noninducing Strain 9
824 (TE-). Red dashed line represents 2-fold increase in copy number. B) Clustering of candidate
825 TEs across strains of *D. virilis*. C) Positive relationship between the copy number of *Penelope*
826 and *Polyphemus* across *D. virilis* strains.
827
828
829 **Figure 2.** Gonad atrophy characteristic of the classic dysgenic phenotype. A) Intrastrain control
830 crosses, intraspecific crosses, and interspecific crosses demonstrating the lack of dysgenesis
831 except in the intraspecific cross. B) Dysgenesis in backcross progeny compared to TE- × TE+
832 cross showing that the F1 males do not induce dysgenesis to the same extent as the pure TE+
833 males. F1-1 are males from the *D. lummei* × TE+ cross and F1-2 males are from the reciprocal
834 cross. The thick red line is the median, and thin red lines the inter-quartile range for each
835 distribution * indicates significantly different from zero ($P<0.05$). ** indicates significant
836 difference between GS and F1 males ($P<0.05$). The dashed line represents the expected effect
837 size based on the two-locus incompatibility models.
838
839 **Figure 3.** The number of progeny produced for each cross demonstrating significantly fewer
840 progeny produced in crosses between *D. lummei* and TE+ in both directions. A) Intrastrain
841 control crosses, intraspecific crosses, and interspecific crosses. B). Backcross progeny compared
842 to the *D. lummei* intrastrain cross showing that the F1 males do not induce progeny lethality, and
843 progeny production is recused. F1-1 are males from the *D. lummei* × TE+ cross and F1-2 males
844 are from the reciprocal cross. The thick red line is the median, and thin red lines the inter-quartile
845 range for each distribution * indicates significantly different from the intrastrain cross of the
846 maternal line ($P<0.05$).
847
848 **Figure 4.** The sex ratio of each cross used to examine deviations from a 50:50 sex ratio caused
849 by sex specific lethality. A) Intrastrain control crosses, intraspecific crosses, and interspecific
850 crosses. B). The sex ratio of backcross progeny showing sex biased progeny ratios occur when
851 *D. lummei* Y is in combination with some complement of TE+ autosomes. F1-1 are males from
852 the *D. lummei* × TE+ cross and F1-2 males are from the reciprocal cross. The thick red line is the
853 median, and thin red lines the inter-quartile range for each distribution * indicates significant
854 deviation from 50:50 sex ratio ($P<0.05$).
855

856

Figure 1

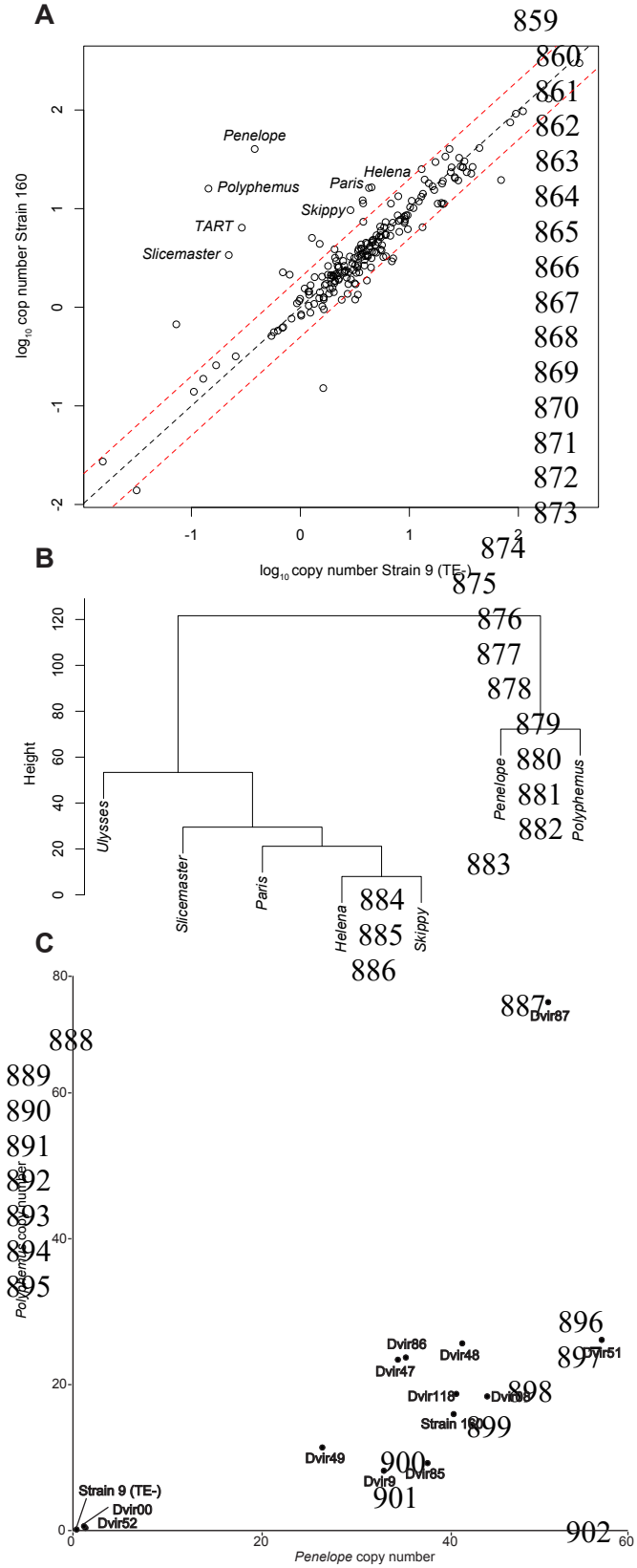
A
Penelope
Polyphemus
Paris
Helena
Skippy
TART
Slicemaster
log10 cop number Strain 160
log10 copy number Strain 9 (TE-)
B
Height
Ulysses
Slicemaster
Paris
Helena
Skippy
Penelope
Polyphemus
C
Dvir87
Dvir86
Dvir48
Dvir47
Dvir51
Dvir118
Dvir49
Dvir9
Dvir85
Strain 9 (TE-)
Dvir00
Dvir52
Penelope copy number

903 **Figure 2**

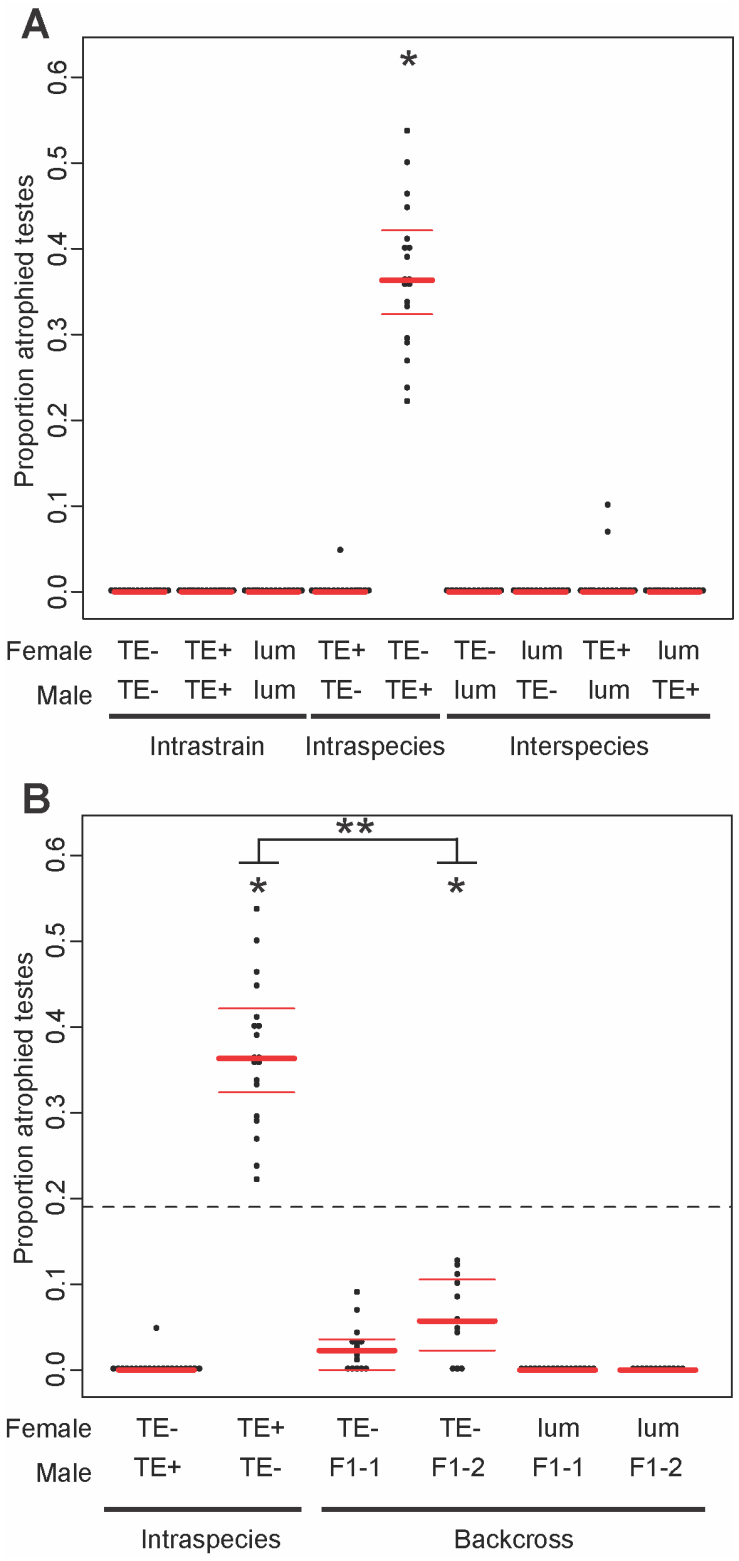

904

905

906 **Figure 3**

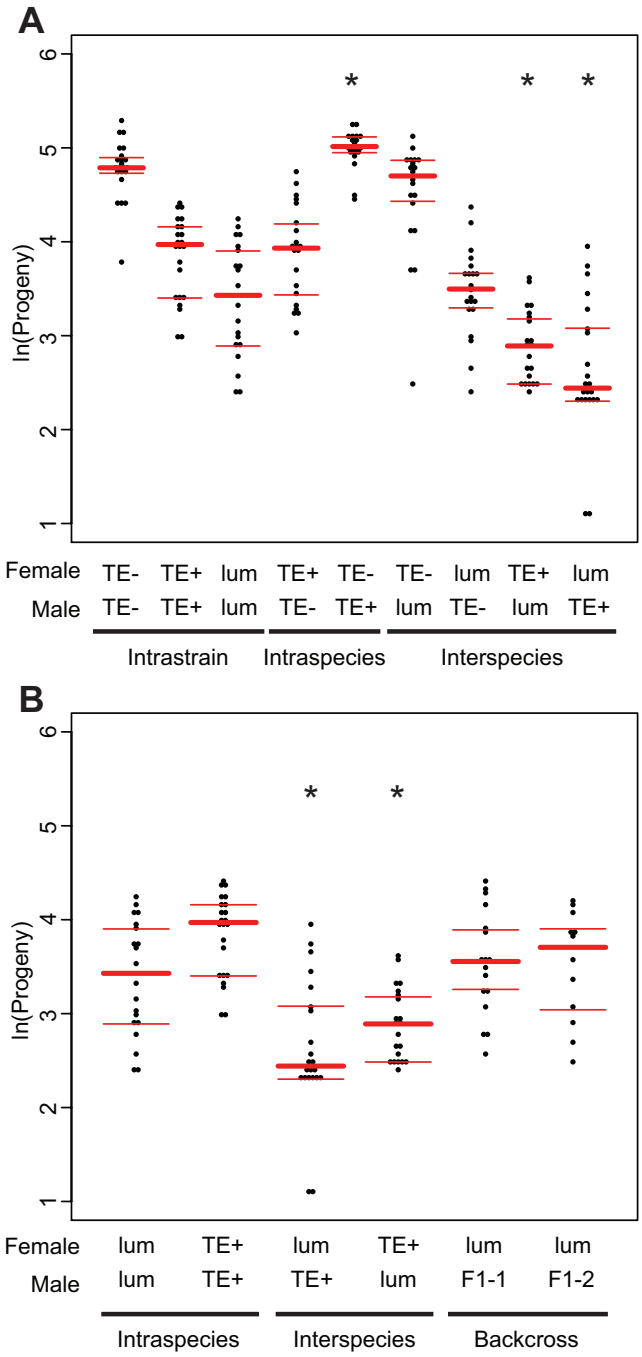

907
908
909
910
911
912
913

914 **Figure 4**

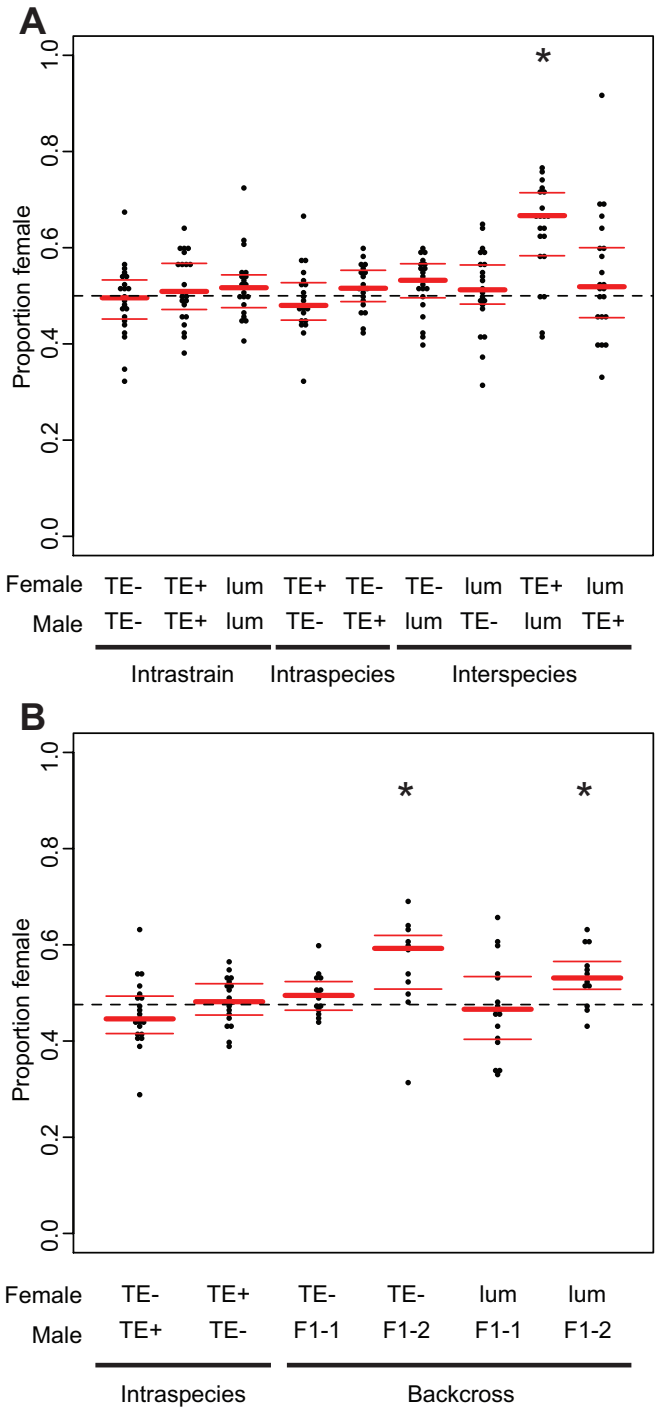

915

916

917